ISSN 1392 - 1207. MECHANIKA. 2010. Nr.1(81)

Investigation of fracture of inhomogeneous cast iron specimens

E. Stupak
Vilnius Gediminas Technical University, Saulėtekio al. 11, 10223 Vilnius-40, Lithuania,
E-mail: Eugenius.Stupak@fm.vgtu.lt

1. Introduction

A major part of fracture mechanics problems [1-4] is related to stress strain fields in the vicinity of discontinuities, cracks, defects, etc. The main methods and techniques are analytical solutions, experimental and numerical.

The analytical models available in the literature allow predicting the stress-strain distribution either within or outside the inhomogeneity and for the further research of the problem. But it is better to use some numerical techniques, because an analytical solutions were obtained generally for simple geometries, e.g. ellipsoidal, cylindrical and spherical voids (cracks) in an infinite domain.

Among the numerical methods the most usually used is the finite element method (FEM). However, it was investigated and shown earlier that it is also necessary to assess the quality of the computed results, which depends on the FE mesh [5] and the assumptions about the stress-strain state [6].

The aim of this paper is the application of FE analysis technique for solving elastic-plastic problem of compact tension (CT) specimen of austempered cast iron. In the previous works [7-9] the analytical and experimental techniques have been described and results of solved elastic problems were discussed.

Murakami [10, 11] investigated interaction effects between small defects and cavities and proposed the simple prediction equation for fatigue limit, which is based on the square root of the equivalent projected area onto the principal stress plane of the defect. Costa et al. [12] proposed an improved technique for fatigue limit of nodular cast irons taking into account the size and positions of graphite nodules.

In the FEM solutions it is possible to account the inhomogeneities, but the solution scale is large since both the matrix and every inhomogeneity should be discretized. In future one may try to compare the obtained results with the results obtained using other techniques, actually boundary element method (BEM), discrete element method (DEM), etc.

In recent years in Lithuania many investigations were devoted for the analysis of different mechanical structures acted of high cycle or low cycle fatigue loading. Stonkus et al. [13] investigated using experiments the welded joints in the high cyclic loading, where the influence of different materials properties in the weld and main material junction (interaction) layer on cracking threshold were analysed.

Jakušovas and Daunys [14] investigated crack opening in the low cycle fatigue case using analytical, experimental and FEM techniques, where the influence of specimen size on crack tip opening displacement contour curve has been taken into consideration.

This paper is organized as follows: problem formulation, description of proposed technique for the calculation of *J*-integral in the vicinity of straight and piecewise linear straight crack front, analysis of obtained numerical results, conclusions and discussion.

2. Problem formulation

The analysis of a CT specimen produced of austempered cast iron, see Fig. 1 (thickness $B = 25$ mm), with an initiated defect and void placed in the different crack front positions is considered below. The size and position of the void has been changed during the investigations.

The external loading F is assumed to be 3.0 kN.

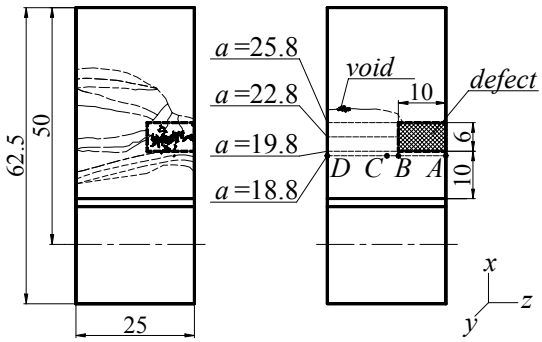

Fig. 1 Geometry and loading of a compact tension specimen

After analyzing the fracture of the CT specimen of cast iron [8], the size and position of the defect in the specimen cross-section, an assumption was made that total dimensions of the defect on fracture surface do not exceed 10x6 mm and the distance to the notch tip is 10 mm. The crack-like defect had been initiated at the model having a rectangle shape as presented in Fig. 1. Few typical crack length values ($a = 18.8$, 19.8, 22.8, 25.8 mm and $a > 25.8$ mm, when the additional void is placed) were chosen alongside a few reference points (A, B, C and D) where stress intensity factor (SIF) was supposed to be indicative.

The behaviour of the specimen's matrix material is assumed to be elastic-plastic. The linear elastic part of the matrix material diagram is characterized by the elasticity modulus $E_1 = 175$ GPa, ratio $\sigma_{01} / E_1 = 0.00171$ and Poisson's ratio $\nu_1 = 0.275$. Behaviour of the material above the yielding limit $\sigma > \sigma_{01} = 300$ MPa is taken as elastic-perfectly plastic.

The behaviour of the specimen's inclusions or voids material (graphite) is assumed to be elastic, characterized by the elasticity modulus $E_2 = 27$ GPa and Poisson's ratio $\nu_2 = 0.275$.

3. Technique for *J*-integral calculation

A novelty technique of path independent *J* integral calculation in piece-wise linear crack front is proposed. Two different *J* integrals can be calculated as surface integrals along contours around: 1) crack tip (line 1-2, J_1 integral path) or 2) defect tip (line 3-4, J_2 integral path) as shown in Fig. 2. *J* integral derives from an energy potential. It was considered the *J* integral along a contour linked to the crack or defect tip which extends by an infinitesimal distance *da* and which takes the contour with it. It was considered the expression of the *J* integral [3]

$$J = \int_{\Gamma} W dy - \int_{\Gamma} T_i \frac{\delta u_i}{\delta x} ds \tag{1}$$

where Γ is any path surrounding the crack tip, *W* is strain energy density (that is, strain energy per unit volume), T_i is traction vector, *u* is displacement vector, *ds* is distance along the path Γ.

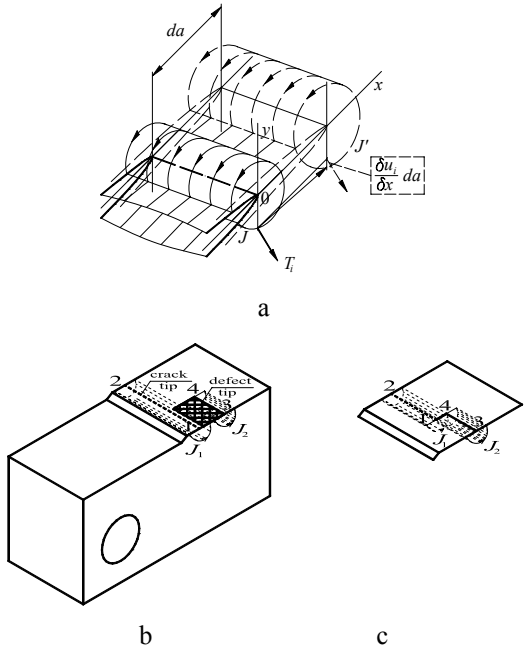

Fig. 2 Illustration of *J* integral investigation: a – at the straight crack front, b – at the proposed piece-wise linear crack front, c – when crack cross defect

During numerical investigations it is better to use the full expression of Eq. (1) [16]

$$J = \int_{\Gamma} W dy - \int_{\Gamma} \left(T_x \frac{\delta u_x}{\delta x} + T_y \frac{\delta u_y}{\delta x} \right) ds \tag{2}$$

where T_x, T_y are traction vectors along *x* and *y* axes respectively ($T_x = \sigma_x n_x + \sigma_{xy} n_y$, $T_y = \sigma_y n_y + \sigma_{xy} n_x$), σ is component stress, *n* is unit outer normal vector to path Γ.

Partition of *J* into elastic and plastic component can be done

$$J = J_{el} + J_{pl} \tag{3}$$

where J_{el} is elastic, J_{pl} is plastic part of *J* integral.

4. Numerical results

ANSYS [15, 16] simulation for a defective model was performed to evaluate the defect and void influence on stress intensity factor and stress-strain state. The FE mesh had been generated using triangular and quadrilateral elements in plane. After they were modified to 3D brick elements, using layers technique. FE mesh used for stress intensity factor calculation, having 25 elements layers through thickness of specimens, is presented in Fig. 3. Only a half of the specimen was investigated using the advantages of symmetry. Less important model volume which is far from the crack tip is meshed with triangle prismatic shape finite elements (56420 nodes, 77170 FE). This helps to thoroughly analyze the stress intensity factor distribution along the crack front and in the vicinity of the defect. FE mesh in the small depth voids volume is finer and had different material properties than others elements.

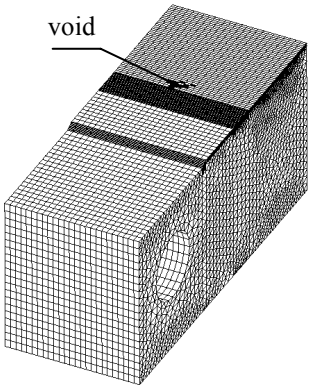

Fig. 3 Finite element mesh of model with void

The numerical accuracy is better the more contour is distant from the crack tip. One must verify that the derived value of *J* is independent of the considered path. Crack extension *da* has been selected as 1% of initial crack length *a*. In order to minimize computational costs and taking into account symmetry only half of specimen was investigated, so the result of *J* integral, obtained by Eq. (2) and/or Eq. (3) must be multiplied by 2.

The distributions of principal stresses in the vicinity of crack and defect tip are illustrated in Fig. 4. Simulation of possible fatigue crack propagation has been done using node releasing technique, which is used instead of remeshing technique. The aim was to determine maximum stress intensity factor (SIF) in the CT specimen. As soon as each elements layer is rather thin, so SIF can be estimated according plane stress assumption using the next formula

$$K = \sqrt{J E_1} \tag{4}$$

where E_1 is modulus of elasticity of matrix material.

SIF values, obtained using Eq. (4), versus accumulated crack length *a* are presented in Fig. 5.

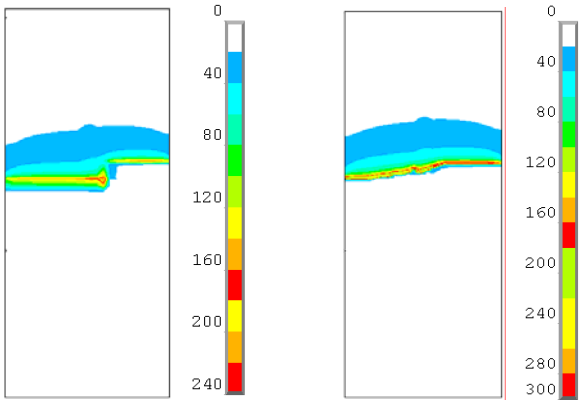

Fig. 4 Principal stresses, MPa in specimen for a typical crack length value $a = 22.8$ mm (a), for $a = 23.9$ mm (b)

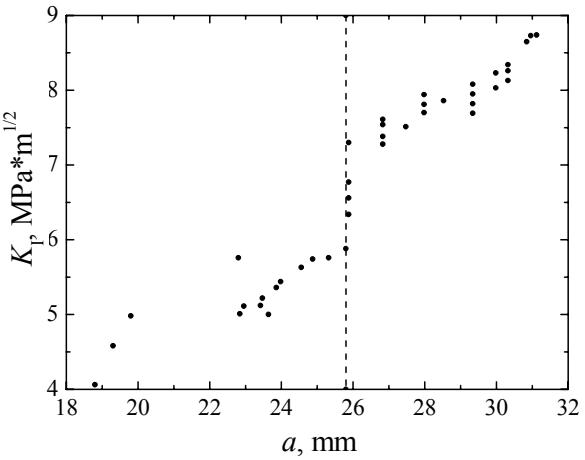

Fig. 5 Stress intensity factor versus accumulated crack length a

The obtained results illustrate SIF changing, when crack length a increased during many numerical tests. Crack length was determined in the all layers through the FE model thickness and then averaged. Taking into account such considerations the different results of K for the different crack fronts with the same averaged crack length a were obtained.

Fig. 5 is separated into 2 parts: 1) when crack length $a < 25.8$ mm only homogeneous matrix material has been taken in the investigation; 2) when crack length $a > 25.8$ mm some additional graphite void is placed. These models were entitled from *void* 1 till *void* 7 and obtained results are presented in the Table.

Void 1 means the defected model (without graphite voids) and was selected for the purpose of comparison. *Void* 2 is the case with graphite voids close to each other and interacted, so their effective area A_{eff}, proposed by Murakami [11], was selected as ≅10 % of defect area. *Void* 3 till *void* 7 have the same A_{eff}, equal to ≅23 % of defect area, but with the different piece-wise linear crack front through the specimen thickness.

Influence of the voids on SIF it is clear from the 5th column, K_{max} increases by 15 % from 7.41 MPa m$^{1/2}$ till 8.74 MPa m$^{1/2}$. The ratio between plastic component J_{pl} of J-integral with result of J-integral increase from 17.7 % till 35.5 %, which explain the J-dominance against K-dominance in the vicinity of crack (void) tip in the elastic-plastic fracture mechanics.

An analysis of SIF distribution through the thickness of the specimen is one of the advantages in 3D FEM analysis. It allows to investigate the influence of any separate void (or even micro-void if the model allows it) on SIF in any part of the specimen in the vicinity of the crack, defect, void, etc. The obtained results of SIF versus specimen thickness B are presented in Fig. 6, where only cases of *void* 1, 2, 5, 7 with increasing K_{max} in the point B (see Fig. 1) are selected for the illustration of results. Maximum value at the defect right point A (distance $t = B$) $K_{max,A} = 5.97$ MPa m$^{1/2}$ in the *void* 7 model. Maximum value at the specimen center point C – $K_{max,C} = 6.15$ MPa m$^{1/2}$ in the *void* 7 model, while at the left specimen edge point D - $K_{max,D} = 5.77$ MPa m$^{1/2}$ in the *void* 2 model.

Table

Summary of main results of investigation

No.	Void effective area A_{eff}, mm^2	Averaged crack length a, mm	Ratio a/W	K_{max}, MPa m$^{1/2}$	J_{pl} / J, %	Stress triaxiality k_{ST}	Homogeneous $\varepsilon_{pl,hom}$	Inhomogeneous $\varepsilon^*_{pl,inh}$
1	2	3	4	5	6	7	8	9
void 1.	0	25.8	0.516	7.41	-	-	-	-
void 2.	6.1	26.8	0.537	7.87	-	-	-	-
void 3.	13.6	29.3	0.587	7.74	-	-	-	-
void 4.	13.6	29.6	0.591	7.76	17.7	0.84	0.00169	0.00162
void 5.	13.6	30.8	0.617	8.65	33.9	0.85	0.00210	0.00180
void 6.	13.6	31.0	0.619	8.73	35.0	0.88	0.00219	0.00190
void 7.	13.6	31.1	0.622	8.74	35.5	0.88	0.00219	0.00190

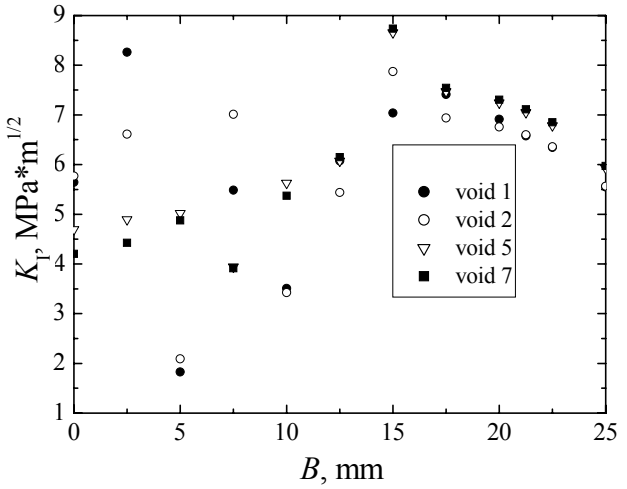

Fig. 6 Stress intensity factor versus specimen thickness B

Some attention must be paid for the zone close to the left specimen edge (distance $t = 0.1B$), where crack length was increased due to the void and the maximum $K_{max,E} = 8.26$ MPa m$^{1/2}$ is only 5.5 % smaller than $K_{max} = 8.74$ MPa m$^{1/2}$. These detailed investigations had proved once more, that voids must be taken into account, especially if their effective area A_{eff} is > than 2.5% of the area of fractured surface.

If the influence of softer material is bigger than in the solved problem one must try to substitute the reduced modulus of elasticity into Eq. (4) instead of E_1. And this is the main advantage of proposed technique in the comparison to other research techniques [11, 12] or standard requirements of ANSYS [16], where material should be homogeneous in the vicinity of the crack.

Graphite is rather soft in comparison with matrix material, so the microcracks will initiate in the matrix connected to graphite. Stress concentration between softer graphite and surface of matrix material will cause plastic strains, after that matrix material fractures. Different material properties will cause so called material mismatching, also the plastic strain mismatch between elastic-perfectly plastic matrix material and elastic graphite material.

During numerical nonlinear analysis plastic values in all the points with different results are averaged in order to satisfy the strain compatibility requirement between elements. Such inequality must be satisfied

$$\varepsilon^{*}_{pl,inh} < \varepsilon_{pl,hom} \tag{5}$$

where $\varepsilon^{*}_{pl,inh}$ is averaged plastic strain for inhomogeneous material, $\varepsilon_{pl,hom}$ is plastic strain for homogeneous material.

This inequality can be transformed into relationship taking into account so called stress triaxiality ratio k_{ST}

$$\varepsilon^{*}_{pl,inh} \cong k_{ST} \cdot \varepsilon_{pl,hom} \tag{6}$$

$$k_{ST} = \frac{\sigma_m}{\sigma_{eqv}} \tag{7}$$

where σ_m is mean stress or hydrostatic pressure, σ_{eqv} is equivalent (von Mises) stress.

Failure of ductile materials is often related to coalescence of microscopic voids. The stress triaxiality is one of the primary factors that influence the coalescence [17, 18].

Contours of equivalent plastic strains for some selected cases (*void* 5 and *void* 7) are presented in Fig. 7, while results are summarised in the 7-9 columns of Table.

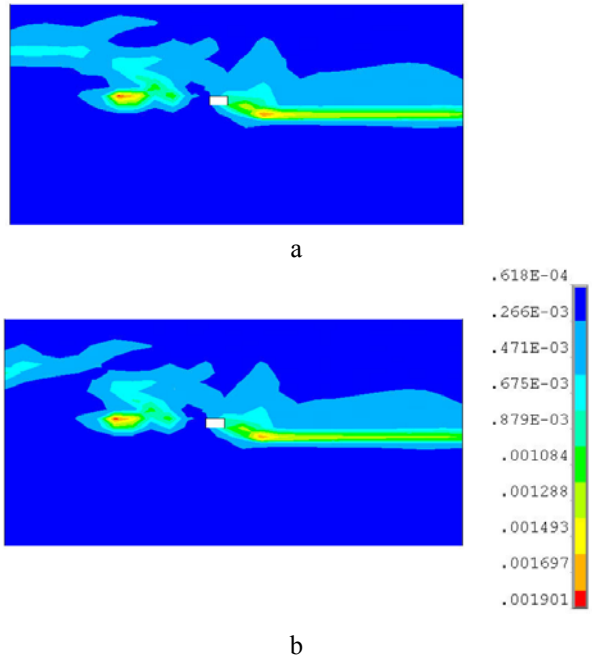

a

b

Fig. 7 Illustration of equivalent plastic strains for: a – *void 5*, b – *void 7*

After performed analysis it can be concluded, that increased stress triaxiality increases the equivalent plastic strains of inhomogeneous material, which maximum value 0.00190 rates to 72 % of total strain equal to 0.00263.

5. Discussion and conclusions

The results of the simulation of inhomogeneous cast iron CT specimen may be summarised as follows:

1. The proposed technique of J-integral calculation allows determination of SIF values through the thickness of the CT specimen with defect and voids and piecewise linear fatigue crack front.
2. The investigation of graphite voids influence on SIF showed increasing by 15 % from 7.41 MPa m$^{1/2}$ (in the specimen without voids) till 8.74 MPa m$^{1/2}$ (including voids – *void* 7 case).
3. Plastic strains in the inhomogeneous specimen were determined using stress triaxiality ratio.

References

1. **Panasiuk, V.V., Andreikiv, A.E., Parton, V.C.** Fundamentals of Fracture Mechanics. Fracture Mechanics and Strength of Materials: Manual.-Kiev: Naukova Dumka, 1988.-488p. (in Russian).
2. **Anderson, T.L.** Fracture Mechanics. Fundamentals and Applications.-Boston: CRC Press, Inc., 1991.-793p.

3. **Miannay, D.P.** Fracture Mechanics.-New-York: Springer, 1998.-337p.
4. **Mróz, Z.** Brittle fracture in plane elements with sharp notches under mixed-mode loading.-J. of Eng. Mechanics, 1997, v.123, No.6, p.535-543.
5. **Kačianauskas, R., Stupak, E., Stupak, S.** Application of adaptive finite elements for solving elastic-plastic problem of SENB specimen. -Mechanika. -Kaunas: Technologija, 2005, Nr.1(51), p.18-22.
6. **Kačianauskas, R., Mróz, Z., Žarnovskij, V., Stupak, E.** Three-dimensional correction of the stress intensity factor for plate with a notch. -Int. J. of Fracture, 2005, v.136, p.75-98.
7. **Leonavičius, M., Bobyliov, K., Krenevičius, A., Stupak, S., Stupak, E.** Evaluation of materials defect influence on fatigue crack threshold. -Kovové materiály: Metallic Materials, 2007, v.45, No.5, p.255-261.
8. **Bobyliov, K., Stupak, E.**, **Leonavičius, M., Stupak, S**. Investigation of the influence of defects on CT specimens fatigue crack. -Proceedings of 13th International Conference „Mechanika-2008“, 3-4 April, 2008, Kaunas, Lithuania, p.67-72.
9. **Leonavičius, M., Bobyliov, K., Krenevičius, A., Stupak, S.** Spheroid graphite cast iron specimens with defects cracking. -Mechanika. -Kaunas: Technologija, 2008, No.1(69), p.13-18.
10. **Murakami, Y.** Stress Intensity Factors Handbook (in 2 volumes). -Elmsford NY (USA): Elsevier, 2001. -3100p.
11. **Murakami, Y.** Metal Fatigue: Effects of Small Defects and Non-Metallic Inclusions. -Oxford: Elsevier science, 2002.-369p.
12. **Costa, N., Machado, N., Silva, F.S.** Influence of graphite nodules on fatigue limit of nodular cast iron. -C. Tech. Materials, 2008, v.20, No.1/2, p.120-127.
13. **Stonkus, R.**, **Leonavičius, M., Krenevičius, A.** Cracking threshold of the welded joints subjected to high cyclic loading. -Mechanika. -Kaunas: Technologija, 2009, No.2(76), p.5-10.
14. **Jakušovas, A., Daunys, M.** Investigation of low cycle fatigue crack opening by finite element method. -Mechanika. -Kaunas: Technologija, 2009, No.3(77), p.13-17.
15. **Thorwald, G, Anderson, T.** Meshing cracks at any locations. -ANSYS Solutions 7, 2006, Issue 2, p.17-20.
16. ANSYS Release 10 Documentation. -SAS IP, Inc., 2008.
17. **Zhang, Y., Chen, Z.** On the effect of stress triaxiality on void coalescence. -Int. J. Fracture, 2007, v.143, p.105-112.
18. **Coppola, T., Cortese, L., Folgorait, P.** The effect of stress invariants on ductile fracture limits in steels.-Eng. Fracture Mechanics, 2009, v.76, p.1288-1302.

E. Stupak

NEVIENALYČIŲ KETAUS BANDINIŲ IRIMO TYRIMAS

R e z i u m ė

Naudojant pasiūlytą *J*-integralo nustatymo nuovarginio dalimis tiesiško plyšio fronte metodiką, atlikti nevienalyčių ketaus bandinių su defektais ir grafito intarpais įtempių intensyvumo koeficiento skaičiavimai.

Ištirta, kaip keičiasi įtempių intensyvumo koeficientas priklausomai nuo plyšio gylio, fronto konfigūracijos, intarpų dydžio ir padėties. Nustatytas 15% įtempių intensyvumo koeficiento prieaugis.

Nevienalyčių ketaus bandinių įtempių analizei naudota BE programa ANSYS.

E. Stupak

INVESTIGATION OF FRACTURE OF INHOMOGENEOUS CAST IRON SPECIMENS

S u m m a r y

The proposed *J*-integral calculation technique in the piece-wise linear fatigue crack front has been used investigating SIF in the inhomogeneous cast iron specimens with defect and graphite voids.

The influence of crack length and front, size and position of voids on SIF have been investigated and the increase of SIF by 15% has been obtained.

Stress-strain state analysis of inhomogeneous cast iron specimens was carried out using FE code ANSYS.

Э. Ступак

АНАЛИЗ РАЗРУШЕНИЯ НЕОДНОРОДНЫХ ЧУГУННЫХ ОБРАЗЦОВ

Р е з ю м е

В работе при помощи предложенной методики для получения *J*-интеграла в окрестности усталостной трещины с кусочно-прямолинейным фронтом рассчитывался коэффициент интенсивности напряжений (КИН) в неоднородных чугунных образцах.

В итоге расследований по влиянию роста трещины, размера и положения частиц графита на КИН, получено 15% увеличение КИН.

Программа КЭ ANSYS была использована для расчета напряженно-деформированного состояния неоднородных чугунных образцов.

Received November 18, 2009
Accepted January 29, 2010